

# GAPDH delivers heme to soluble guanylyl cyclase

Received for publication, April 9, 2020, and in revised form, April 28, 2020 Published, Papers in Press, April 30, 2020, DOI 10.1074/jbc.RA120.013802

Yue Dai , Elizabeth A. Sweeny , Simon Schlanger, Arnab Ghosh , and Dennis J. Stuehr\* 

From the Department of Inflammation and Immunity, Lerner Research Institute, The Cleveland Clinic, Cleveland, Ohio, USA

Edited by Ruma Banerjee

Soluble guanylyl cyclase (sGC) is a key component of NO–cGMP signaling in mammals. Although heme must bind in the sGC  $\beta$ 1 subunit (sGC $\beta$ ) for sGC to function, how heme is delivered to sGC $\beta$  remains unknown. Given that GAPDH displays properties of a heme chaperone for inducible NO synthase, here we investigated whether heme delivery to apo-sGC $\beta$  involves GAPDH. We utilized an sGC $\beta$  reporter construct, tetra-Cys sGC $\beta$ , whose heme insertion can be followed by fluorescence quenching in live cells, assessed how lowering cell GAPDH expression impacts heme delivery, and examined whether expressing WT GAPDH or a GAPDH variant defective in heme binding recovers heme delivery. We also studied interaction between GAPDH and sGC $\beta$  in cells and their complex formation and potential heme transfer using purified proteins. We found that heme delivery to apo-sGC $\beta$  correlates with cellular GAPDH expression levels and depends on the ability of GAPDH to bind intracellular heme, that apo-sGC $\beta$  associates with GAPDH in cells and dissociates when heme binds sGC $\beta$ , and that the purified GAPDH–heme complex binds to apo-sGC $\beta$  and transfers its heme to sGC $\beta$ . On the basis of these results, we propose a model where GAPDH obtains mitochondrial heme and then forms a complex with apo-sGC $\beta$  to accomplish heme delivery to sGC $\beta$ . Our findings illuminate a critical step in sGC maturation and uncover an additional mechanism that regulates its activity in health and disease.

Soluble guanylyl cyclase (sGC, EC 4.6.1.2) responds to NO to generate cGMP, which acts as a second messenger molecule in numerous biological settings (1–3). Disruption of sGC activity is tied to a spectrum of pulmonary, cardiovascular, and neurodegenerative diseases (4–6). The mature sGC enzyme is a heterodimer comprised of an  $\alpha$  subunit and a  $\beta$  subunit, and only the sGC $\beta$  subunit contains a binding site for iron protoporphyrin IX (heme) (7). When NO binds to the sGC $\beta$  heme, it triggers protein conformational changes that activate cGMP production by the sGC heterodimer (8–11). Thus, cell heme delivery and insertion processes are critical for allowing sGC to mature and function in numerous NO-driven cGMP signaling cascades (12).

Although sGC structure and function have been studied for decades, the processes that form a functional sGC $\alpha/\beta$  heterodimer are only beginning to be understood (2, 7, 12–14). This includes the intracellular pathways that transport and insert heme into the immature apo-sGC $\beta$  (12). We know that the chaperone Hsp90 participates in sGC maturation by bind-

ing directly to apo-sGC $\beta$ . Its binding prevents apo-sGC $\beta$  from forming a heme-free sGC $\alpha/\beta$  heterodimer and also enables heme insertion into apo-sGC $\beta$  in an ATP-dependent process (15, 16). However, how heme is delivered to apo-sGC $\beta$  remains unclear.

To address this question, we investigated whether heme delivery to apo-sGC $\beta$  might rely on GAPDH. This idea stems from our recent finding that GAPDH behaves like a heme chaperone to deliver heme to at least one mammalian protein, the inducible NO synthase (17). Here we performed mammalian cell culture studies with HEK293 cells using the reporter tetra-Cys sGC $\beta$  construct (TC-sGC) (18), whose in-cell fluorescence can be used to follow its heme delivery. We also performed experiments with purified proteins to assess their potential for direct interaction and heme transfer. Our findings reveal that mitochondrially generated or exogenously added hemes are delivered to apo-sGC $\beta$  in mammalian cells through a GAPDH-dependent process that likely involves heme transfer from GAPDH to apo-sGC $\beta$ .

## Results

### *Delivery of exogenous heme to apo-sGC $\beta$ correlates with the GAPDH expression level and the heme binding ability of GAPDH*

To generally assess GAPDH involvement in heme delivery, we developed the following cell culture strategy. We first tested whether siRNA knockdown of GAPDH expression reduces heme acquisition by the target protein. If affirmative, then we tested whether the target's heme insertion can be rescued in the knockdown cells by transiently expressing siRNA-resistant forms of WT GAPDH or a H53A GAPDH heme binding–defective variant that is unable to bind intracellular heme in mammalian cells (17). If only WT GAPDH could rescue the heme insertion, then we scored the target protein as having GAPDH-dependent heme delivery.

We applied this approach to sGC. HEK293 cells were initially heme-depleted by culturing with the heme biosynthesis inhibitor succinyl acetone (SA) (19) before being transiently transfected to express our TC-sGC $\beta$  reporter protein. Cell heme depletion ensures that heme-free (apo) TC-sGC $\beta$  will be expressed. The TC-sGC $\beta$  incorporates a TC motif near its heme-binding site that can bind the indicator dye FAsH and become fluorescent. Its fluorescence undergoes quenching when heme binds. In some cases, knockdown cells were cotransfected with siRNA-resistant and HA-tagged expression constructs of WT GAPDH (HA-GAPDH) or the GAPDH heme binding–defective variant (HA-GAPDH H53A). After 24 h, the expressed apo-TC-sGC $\beta$  was labeled with the FAsH reagent,

This article contains [supporting information](#).

\* For correspondence: Dennis J. Stuehr, [stuehrd@ccf.org](mailto:stuehrd@ccf.org).

## GAPDH delivers heme to sGC

heme was added to the cell cultures, and then we assessed heme insertion into FIAsh-labeled apo-TC-sGC $\beta$  by monitoring cell fluorescence over a 3-h period (heme insertion causes quenching of FIAsh fluorescence).

Control cell cultures that received no heme but were labeled with FIAsh maintained steady fluorescence intensity over the time course of the reading. Those that also received heme showed a steady loss in fluorescence, indicating that FIAsh-labeled apo-TC-sGC $\beta$  steadily incorporated heme within 2 h (Fig. 1A). In cells that did undergo GAPDH knockdown treatment, there was loss of GAPDH expression, as confirmed by Western blot analysis (Fig. 1C), and these cells showed comparatively little fluorescence loss after heme addition (Fig. 1A). Thus, diminished GAPDH expression correlated with poor heme delivery to apo-TC-sGC $\beta$ . Notably, normal heme delivery in knockdown cells was restored by coexpression of WT HA-GAPDH but not by coexpression of the HA-GAPDH H53A heme binding-defective variant (Fig. 1B). We conclude that heme delivery to apo-TC-sGC $\beta$  correlates with the cell's GAPDH expression level and depends on the heme binding ability of GAPDH.

### Delivery of mitochondrial heme to apo-TC-sGC $\beta$ correlates with the GAPDH expression level and the heme binding ability of GAPDH

Because mitochondria are the natural source of biosynthetic heme in mammalian cells, we next tested whether delivery of mitochondrially generated heme to apo-TC-sGC $\beta$  depends on GAPDH. We performed cell culture experiments as described above but added the natural heme precursors ferric citrate (Fe-cit) and  $\delta$ -aminolevulinic acid ( $\delta$ -ALA) to the cells in place of added heme. When added to cells, these precursors are converted into heme by mitochondria (20, 21). Because SA inhibits the  $\delta$ -ALA-converting enzyme, we changed the culture medium to remove SA prior to adding the heme precursors.

In heme-depleted HEK293 cells expressing FIAsh-labeled apo-TC-sGC $\beta$ , adding Fe-cit +  $\delta$ -ALA caused a decrease in fluorescence after a short delay (Fig. 2A). This indicated that, after cells had converted the precursors into heme, they delivered it to apo-TC-sGC $\beta$ . Heme delivery was inhibited in cells with GAPDH expression knocked down (Fig. 2A) and rescued in knockdown cells by expression of HA-GAPDH WT but not by the HA-GAPDH H53A heme binding-defective variant (Fig. 2B). Fig. 2C shows that knockdown lowered native GAPDH expression in cells and that the TC-sGC $\beta$  expression levels were similar under the various experimental conditions. Thus, cell delivery of mitochondrial heme to apo-TC-sGC $\beta$  also correlates with the expression level of GAPDH and depends on its ability to bind intracellular heme.

### Confirmation that adding exogenous heme or the heme precursors increases intracellular heme levels

To confirm the intended effect of adding heme or the heme precursors to our HEK293 cells, we utilized a recently characterized fluorescent protein, HS1, which can sense and report the intracellular heme level (22, 23). The sensor contains a red

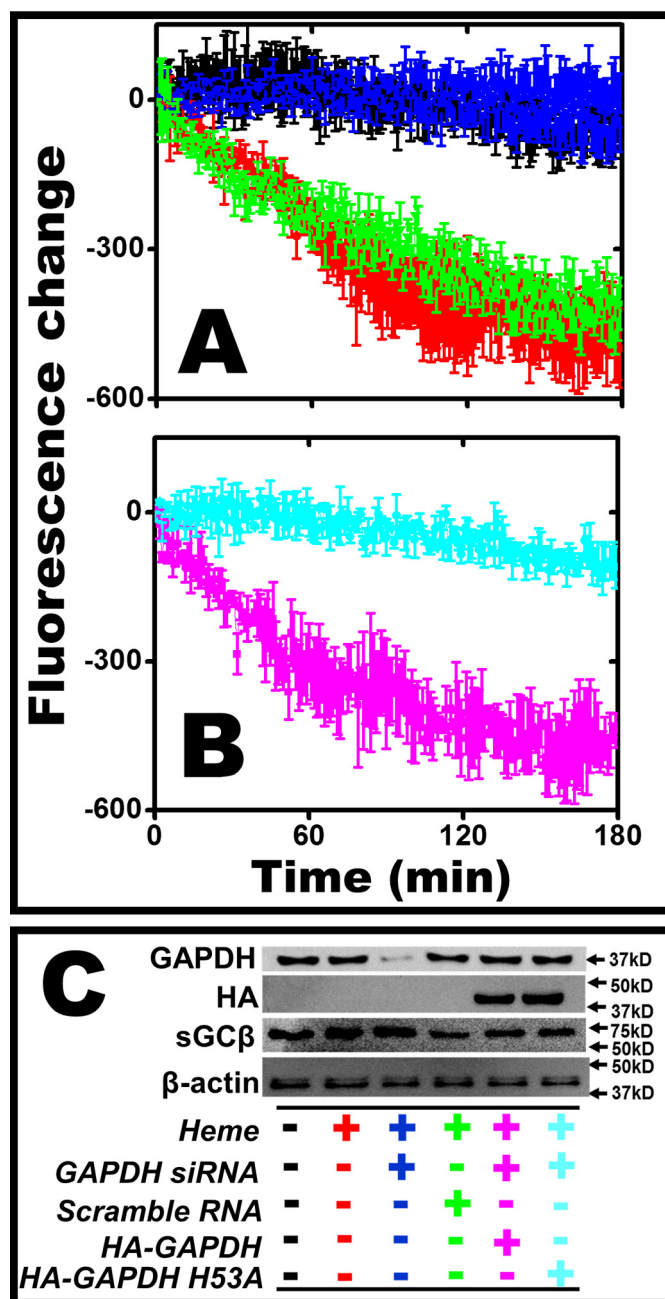


**Figure 1. Heme delivery to apo-TC-sGC $\beta$  correlates with the GAPDH expression level and heme binding property of GAPDH.** apo-TC-sGC $\beta$ 1 was expressed in heme-deficient HEK293 cells and FIAsh-labeled. In some cases, cells also received transfections with GAPDH siRNA or scrambled siRNA along with HA-tagged GAPDH constructs; all are color-indicated in C. Fluorescence was monitored over time after adding buffer or 5  $\mu$ M heme to cell cultures. Fluorescence quenching indicates heme delivery to FIAsh-apo-sGC $\beta$ . A, the effects of heme addition and of knockdown of GAPDH expression. B, the capacity of HA-GAPDH or HA-GAPDH H53A expression to rescue heme delivery in GAPDH knockdown cells. C, representative Western blots indicating the relative expression levels of the indicated proteins in the cell supernatants. The fluorescent kinetic traces of A and B are the mean  $\pm$  S.D. of three wells and are representative of three independent experiments.

(mKATE2) and a green (eGFP) fluorescent protein positioned in tandem with a cytochrome *b* heme-binding fragment (22, 23). Only GFP fluorescence is quenched upon heme binding, and so the GFP:mKATE2 fluorescence ratio is a measure of sensor heme occupancy. This sensor is used to detect and quan-

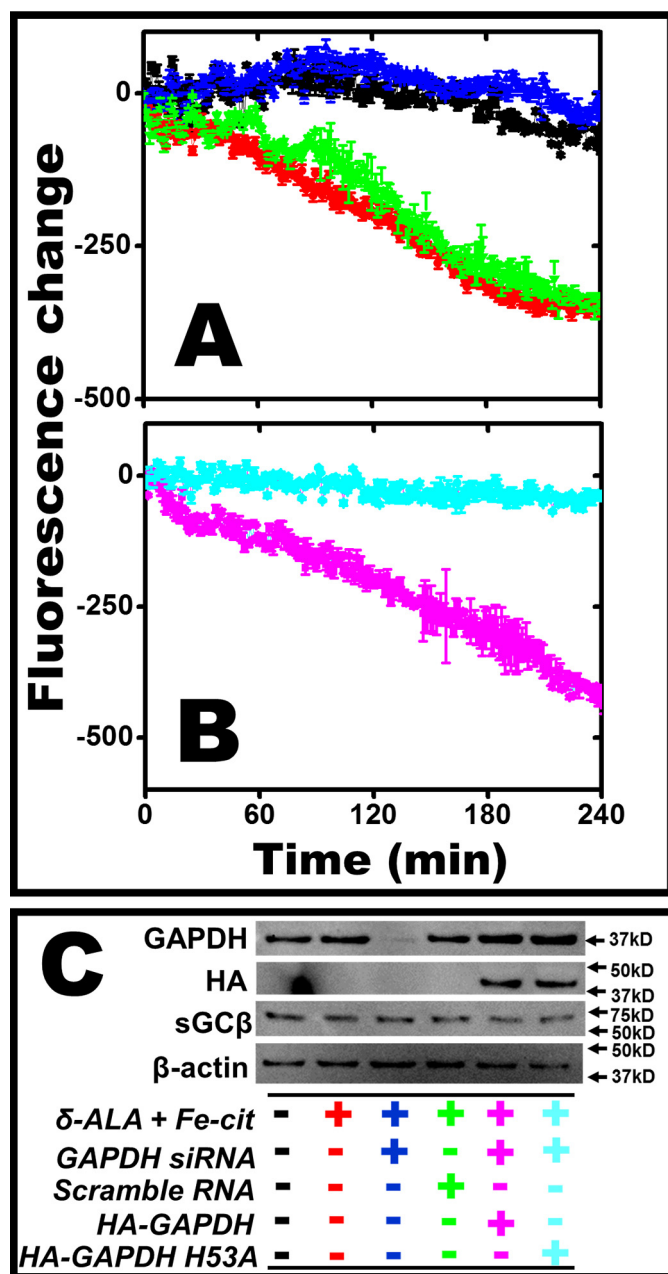


**Figure 2. GAPDH delivers mitochondrially produced heme to apo-TC-sGC $\beta$ .** apo-TC-sGC $\beta$  was expressed in heme-deficient HEK293 cells and FlAsH-labeled. In some cases, cells also were transfected with GAPDH siRNA or scrambled siRNA along with HA-tagged GAPDH constructs; all are color-indicated in C. Fluorescence was monitored with time after adding buffer or 500  $\mu$ M  $\delta$ -ALA plus 200  $\mu$ M Fe-cit to cell cultures. Fluorescence quenching indicates heme delivery to FlAsH-apo-sGC $\beta$ . A, the effects of  $\delta$ -ALA + Fe-cit addition and of knockdown of GAPDH expression. B, the capacity of HA-GAPDH or HA-GAPDH H53A expression to rescue heme delivery in GAPDH knockdown cells. C, representative Western blots indicating the relative expression levels of the indicated proteins in the cell supernatants. The fluorescent traces of A and B are the mean  $\pm$  S.D. of three wells and are representative of three independent experiments.

tify labile heme levels in cells in several settings (17, 22). Fig. S1 shows the results of a representative cell sorting experiment we performed in which HEK293 cells expressing the heme sensor were given nothing, Fe-cit +  $\delta$ -ALA, or heme for 3 h prior to analysis. The added heme or Fe-cit +  $\delta$ -ALA caused a leftward shift in cell distributions regarding their GFP:mKATE2 fluores-

cence ratio. The leftward shift indicates that the heme sensor increased its heme saturation level (22), confirming that adding heme or the heme precursors to HEK293 cells causes them to increase their intracellular heme level.

#### sGC maturation to a functional heterodimer correlates with GAPDH expression and its heme binding property

To extend our results within the context of normal sGC maturation, we measured how similar experimental manipulations of cell GAPDH expression would impact the development of NO-responsive sGC activity. Because NO can only activate the mature heme-containing sGC heterodimer, measuring NO-triggered cGMP biosynthesis activity is a functional measure of successful heme delivery to apo-sGC $\beta$  (16).

HEK293 cells were grown under normal conditions (not heme-depleting) and were transfected to express sGC $\alpha$  and sGC $\beta$ . They also had their GAPDH expression altered using siRNA knockdown with or without transfection of either of the HA-tagged GAPDH proteins, as described above. We then gave the cells the NO donor *N*-ethyl-2-(1-ethyl-2-hydroxy-2-nitrosylhydrazino) ethanamine (NOC12) or gave them the sGC activator BAY58-2667 (BAY58) for 30 min to activate their sGC cGMP production. The NO donor can only activate heme-containing sGC, whereas BAY58 can only activate heme-free sGC (24). Thus, measuring the extent of BAY58 activation serves to independently assess the degree of heme insertion into apo-sGC $\beta$ , but in an inverse manner relative to the results obtained with the NO donor.

As illustrated in Fig. 3, cells that were transfected to express sGC $\alpha$  and sGC $\beta$  but otherwise had no other manipulations (untreated) developed cGMP synthesis activity that was responsive to the NO donor and to BAY58. This confirms previous reports that cells generate a mixture of heme-containing and apo-sGC $\beta$  when they are grown under normal culture conditions (16, 25, 26). Knockdown of cell GAPDH expression by siRNA treatment was confirmed by Western blot analysis (Fig. 3B) and found to inhibit development of NO-responsive cGMP activity and increase development of BAY58-responsive activity. This indicates that GAPDH knockdown caused the cells to generate a greater proportion of sGC $\beta$  in its heme-free form. In comparison, transfecting cells with a scrambled siRNA caused little or no change in their NO *versus* BAY58 activation responses relative to untreated cells. Notably, expressing HA-GAPDH WT in GAPDH knockdown cells, but not the H53A HA-GAPDH heme-binding defective variant, reversed the changes because of GAPDH knockdown so that the NO *versus* BAY58 activity profile essentially matched that of the untreated or the scrambled siRNA-treated cells. Together, these activity measurements indicate that delivery of mitochondrial heme to apo-sGC $\beta$  during normal sGC heterodimer maturation is GAPDH-dependent; it correlates with the cell's GAPDH expression level and with the ability of GAPDH to bind intracellular heme.

#### GAPDH and sGC $\beta$ associate in cells

Because GAPDH dependent heme delivery to apo-sGC $\beta$  could involve their in-cell association, we investigated under which circumstances sGC $\beta$  might associate with GAPDH in

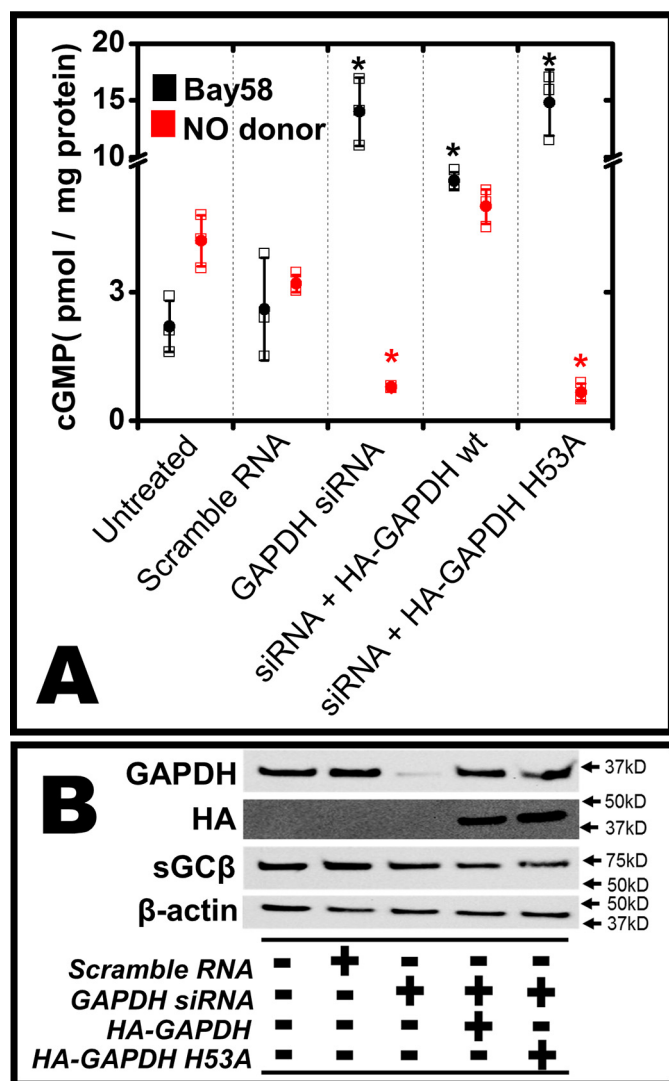


**Figure 3. GAPDH expression level and heme binding property correlate with maturation of sGC activity.** HEK293 cells were cultured in normal medium and transfected to express sGC $\alpha$ 1 and sGC $\beta$  along with cotransfection with the various siRNA and HA-GAPDH vectors as indicated. The GTP cyclase activities of cell supernatants were measured in response to the NO donor NOC12 or to BAY58, which activate mature heme-containing sGC versus immature heme-free sGC, respectively. *A*, comparative cyclase activities, with y axes colored to match bars. *B*, representative Western blot showing the protein expression levels in cell supernatants under the indicated culture conditions. Activity values are the mean  $\pm$  S.D. (error bars) of three measurements and are representative of three experiments each. \*,  $p < 0.05$ ; change in activity relative to no-treatment control cultures.

cells. We performed immunoprecipitation (IP) on supernatants made from heme-deficient HEK293 cells that expressed apo-sGC $\beta$ . Cells were lysed at various times after adding heme to the cultures. Fig. 4 shows that GAPDH and apo-sGC $\beta$  were associated at the time of heme addition, but their association began to drop off after 15 min of culture with heme and was practically undetectable after 3 h. A similar sGC $\beta$  association–dissociation pattern was observed with the chaperone Hsp90 (Fig. 4), which is known to bind with apo-sGC $\beta$  to help drive its heme insertion and then become released (19, 25, 27). Our results indicate that GAPDH associates with apo-sGC $\beta$  in cells prior to and during the heme insertion process and then dissociates when heme insertion is complete.

### GAPDH and a GAPDH–heme complex can directly bind with apo-sGC $\beta$

We next probed whether purified sGC $\beta$  and GAPDH could form a direct complex and whether heme bound in either protein would influence their ability to do so. A set concentration of FITC-labeled sGC $\beta$  protein (0.5  $\mu$ M) was titrated with increasing amounts of GAPDH, and their binding was assessed by measuring residual fluorescence polarization, which increases upon protein complex formation because of the complex having a slower tumbling rate (19). Fig. 5A shows that GAPDH bound to apo-sGC $\beta$  at lowmicromolar concentrations and in a saturable manner, whereas sGC $\beta$  that was heme-replete was much less prone to bind with GAPDH. On the other hand, we observed that heme-free and heme-bound GAPDH (at one heme per GAPDH tetramer) could bind with near-equal affinity to an apo-sGC $\beta$  heme binding–defective variant (apo-sGC HD) (28) (Fig. 5B). We utilized this variant in place of WT apo-sGC $\beta$  to eliminate any potential complications caused by a heme transfer occurring during the experiment. Together, our studies show that heme-free or heme-bound GAPDH can form a direct complex with apo-sGC $\beta$ , but GAPDH does not do so when the sGC $\beta$  already contains a bound heme.

### The GAPDH–heme complex transfers heme to apo-sGC $\beta$

Given the above, we examined whether the GAPDH–heme complex could transfer heme to apo-sGC $\beta$ . We mixed the GAPDH–heme complex with an equimolar amount of FLAsH-labeled apo-TC-sGC $\beta$  protein at concentrations that allow their binding to form a complex. This resulted in heme transfer to FLAsH-labeled apo-TC-sGC $\beta$ , as indicated by loss in fluorescence intensity, which neared completion by around 200 s (Fig. 6). The kinetic traces were fit to a single exponential equation (Fig. 6) and gave a mean heme transfer rate of  $9.2 \pm 3.7 \times 10^{-3} \text{ s}^{-1}$  ( $n = 3$ ). In comparison, no fluorescence loss was seen in an identical experiment that used FLAsH-labeled apo-TC-sGC $\beta$  HD variant (Fig. 6). Thus, heme transfer occurred from the GAPDH–heme complex and depended on the apo-sGC $\beta$  recipient having a functional heme binding site.

### Discussion

To engage in NO–cGMP signaling, mammalian cells must first form a heme-containing sGC heterodimer. We found that cell heme delivery to apo-sGC $\beta$  is GAPDH-dependent; it correlates with the GAPDH expression level and relies on the specific ability of GAPDH to bind intracellular heme. These results, when combined with our findings using purified proteins, argue that GAPDH functions to deliver heme to apo-sGC $\beta$  during sGC maturation in cells.

Besides illuminating a fundamental step in the biogenesis of NO–cGMP signaling, our study makes the following five advances.

- 1) It identifies sGC as the second protein to have GAPDH-dependent heme delivery. This is important from a GAPDH point of view because it shows that its heme delivery function is not restricted to inducible nitric oxide synthase (iNOS) and instead also operates for a completely unrelated protein. This implies that GAPDH probably plays a broader role as a heme chaperone. The fact that the new client is sGC is also important

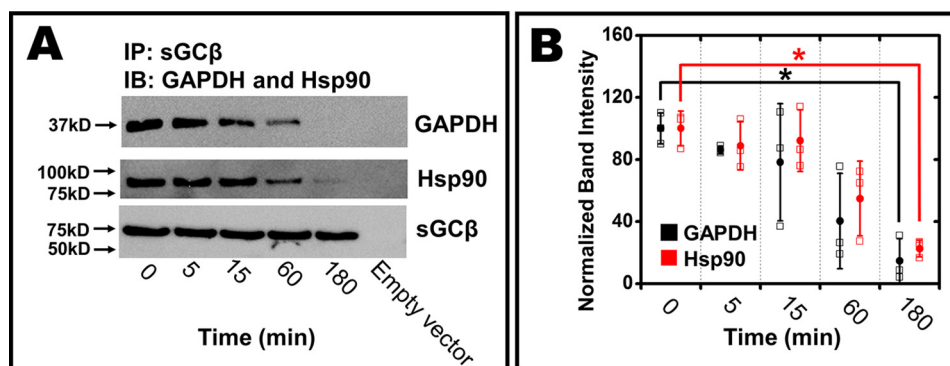


**Figure 4.** GAPDH associates with apo-sGC $\beta$  in cells prior to and during heme delivery. Heme-deficient HEK293 cells expressing apo-sGC $\beta$  were given 5  $\mu$ M heme, and then supernatants (500  $\mu$ g of total cell supernatant protein) were prepared at the indicated time points and subjected to IP. *A*, representative Western blots indicating the relative amounts of Hsp90, GAPDH, and sGC $\beta$  in the IP at each time point. *B*, densitometric quantification of Hsp90 and GAPDH in the IPs. Values are the mean  $\pm$  S.D. of three independent experiments and are compared with  $t = 0$  values for significance determination; \*,  $p < 0.05$ . *IB*, immunoblot.

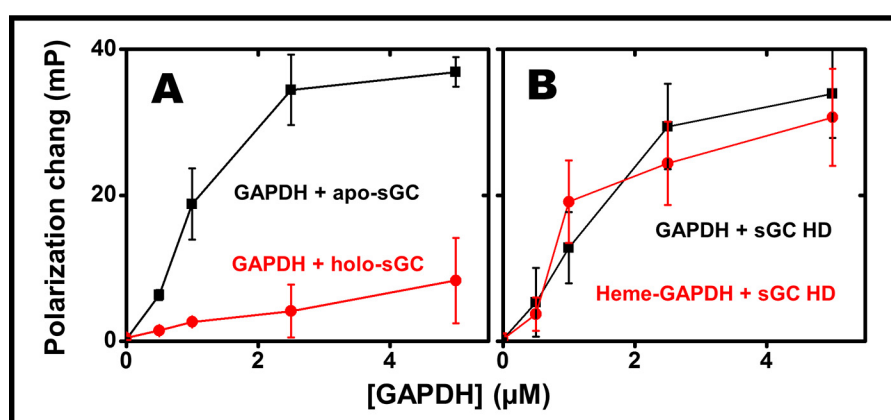


**Figure 5.** GAPDH binding to sGC $\beta$  and the effect of bound heme. *A*, FITC-labeled apo-sGC $\beta$  or holo-sGC $\beta$  (0.5  $\mu$ M) was titrated with GAPDH, and the change in FITC residual polarization was measured (increase = complex formation). *B*, FITC-labeled apo-sGC $\beta$  HD (heme binding-defective, 0.5  $\mu$ M) was titrated with GAPDH or a GAPDH-heme complex. Points are the mean  $\pm$  S.D. for three samples and are representative of two independent experiments.

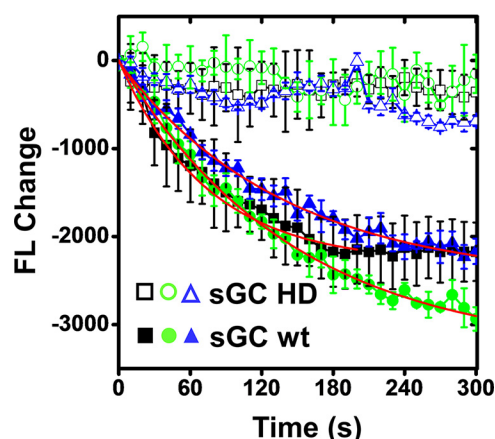


**Figure 6.** Kinetics of GAPDH heme transfer to apo-TC-sGC $\beta$ . FIAsh-labeled apo-TC-sGC $\beta$  WT or a HD mutant (5  $\mu$ M) were given 5  $\mu$ M GAPDH-heme complex (one heme per GAPDH tetramer) at 25  $^{\circ}$ C, and fluorescence (*FL*) was recorded over time. A fluorescence decrease indicates heme transfer and binding within apo-TC-sGC $\beta$ . The different symbols indicate independent experiments. Each point is the mean  $\pm$  S.D. for three replicates. Red lines show the data fit to a single exponential decay equation and give heme transfer rates of  $1.35 \times 10^{-2} \text{ s}^{-1}$ ,  $6.88 \times 10^{-3} \text{ s}^{-1}$ , and  $7.19 \times 10^{-3} \text{ s}^{-1}$ .

because of its widely appreciated biomedical and pharmacologic significance (1–6).

2) It describes a general method to determine whether any heme protein has GAPDH-dependent heme delivery. In our

previous paper on GAPDH and iNOS (29), we struggled with the impact of the cells' native GAPDH expression level, which ultimately buffered how expressing the H53A GAPDH heme binding-defective variant impacted cell heme delivery to iNOS. Here we describe a combined siRNA GAPDH expression knockdown and siRNA-resistant GAPDH expression rescue protocol using WT GAPDH *versus* the heme binding-defective variant. Proceeding this way, we obtained a reduced background of native GAPDH expression, which, in turn, allowed us to clearly test for GAPDH-dependent heme delivery. The same approach can investigate heme delivery to other proteins.

3) It is the first to show that GAPDH delivers mitochondrial heme to a client protein. In our previous paper (17) we showed that mitochondrial heme loads onto GAPDH but did not show that it is transferred to apo-iNOS. Here we showed that GAPDH delivers mitochondrial heme to apo-sGC $\beta$  after the cells were given mitochondrial heme precursors and also when the cells were cultured under normal conditions and not given any heme precursors. Our finding that GAPDH delivers heme from the natural source (mitochondria) is an improvement over our previous and current demonstrations that GAPDH delivers heme that was exogenously added to the cells, which is an experimentally convenient but artificial means of heme acquisition.

## GAPDH delivers heme to sGC

4) It determines the rules of engagement between GAPDH and sGC $\beta$  in cells and in their purified forms. We show that the two proteins associate in cells and that the two purified proteins can have a direct binding interaction. Their interaction occurs according to certain rules. To interact with GAPDH, sGC $\beta$  cannot have heme bound, whereas GAPDH or its heme complex can interact well with apo-sGC $\beta$ . These findings are significant because they point toward a mechanism of action; namely, that GAPDH as a heme-bound entity can bind directly with apo-sGC $\beta$  and may possibly function this way for heme delivery.

5) It is the first to observe and kinetically characterize actual heme transfer from a GAPDH–heme complex to a client protein. Observing direct heme transfer from GAPDH to apo-sGC $\beta$  is important because it informs on the possible mechanism and provides a framework for further molecular studies.

To probe for GAPDH involvement, we used targeted protein knockdown to diminish the expression of native GAPDH in the cells, and then we rescued expression with a WT GAPDH or a heme binding–defective variant. It is conceivable that knocking down GAPDH expression could indirectly diminish cell heme delivery by impacting other functions of GAPDH; notably, its dehydrogenase activity for cell glycolysis. This potential effect of GAPDH knockdown was considered and dismissed in our earlier study of GAPDH involvement in iNOS heme delivery (29). Moreover, if this were the case, then, in this study, we should have observed rescue of heme delivery when the H53A GAPDH variant was expressed in knockdown cells because this mutant is known to have normal GAPDH dehydrogenase activity (17). Instead, we suspect that lowering the GAPDH expression level inhibits cell heme delivery because it lowers the cell's pool of the GAPDH–heme complex, which likely represents the portion of cellular heme that is available for heme delivery to apo-sGC $\beta$  and to other GAPDH-dependent proteins like iNOS.

When GAPDH interacted with sGC $\beta$  in cells or in purified form, it favored apo-sGC over heme-replete sGC $\beta$ . Indeed, GAPDH dissociated from sGC $\beta$  in cells during the later stage of the heme insertion process. This behavior is exactly what one would expect if GAPDH functions to deliver heme to apo-sGC $\beta$ .

We also saw that heme transfer occurred when the purified GAPDH–ferric heme complex was mixed with an equimolar amount of apo-sGC $\beta$  under conditions that allowed them to form a complex. As noted above, this represents the first direct demonstration of heme transfer from a GAPDH–heme complex to any client apo-protein. Granted, heme transfer occurring under this circumstance might be expected because the relative ferric heme binding affinities favor heme binding in apo-sGC $\beta$  over GAPDH. The estimated GAPDH ferric heme  $K_d$  is 150 nM (17), whereas the ferric heme  $K_d$  of sGC $\beta$  may range from 3 to 55  $\mu$ M, as calculated using the reported heme  $k_{on}$  of  $2.8 \times 10^6 \text{ M}^{-1} \text{ s}^{-1}$  (30) and the reported  $k_{off}$  measures (31, 32). Having an intermediate heme  $K_d$  makes sense if GAPDH is to function in cell heme delivery because it would allow GAPDH to load heme and then transfer it to downstream higher-affinity clients, like apo-sGC $\beta$  or apo-iNOS.

We also found that the rate of ferric heme transfer from GAPDH to apo-sGC $\beta$  ( $9.2 \times 10^{-3} \text{ s}^{-1}$ ) is about three times faster than the reported heme  $k_{off}$  of GAPDH ( $2.8 \times 10^{-3} \text{ s}^{-1}$ ), which was determined previously at the same temperature and in the presence of a 10-fold excess of apo-myoglobin (17). This rate difference argues that the interaction between the GAPDH–heme complex and apo-sGC $\beta$  promotes heme transfer beyond what would occur because of simple heme dissociation from GAPDH. It will now be possible to study the molecular nature of the interaction between the GAPDH–heme complex and apo-sGC $\beta$  and how it enables intracellular heme delivery to apo-sGC $\beta$ .

Our results and previous studies suggest a working model for the heme delivery, heme insertion, and related steps that occur during maturation of a functional sGC heterodimer in cells (Fig. 7). In the immature state, apo-sGC $\beta$  is in complex with Hsp90 and cannot bind an sGC $\alpha$  subunit to form a heterodimer (16, 19). Heme that enters the cell cytosol, potentially via the mitochondrial heme exporter FLVCR1b (33) or via import of exogenous heme through the cell membrane, and binds to GAPDH through a still to be determined process to ultimately generate a pool of safely sequestered and bioavailable heme in the cell. The GAPDH–heme complex may then bind to the Hsp90–apo-sGC $\beta$  complex to enable heme transfer. Heme insertion into apo-sGC $\beta$  then proceeds in an Hsp90- and ATP-dependent process (12). Heme insertion into apo-sGC $\beta$  likely promotes conformational changes that favor dissociation of Hsp90 and GAPDH from heme-replete sGC $\beta$ , which, in turn, enables it to bind with an sGC $\alpha$  partner subunit and form a heme-containing functional sGC heterodimer (19). This model introduces some new concepts and provides a framework for further investigation.

Our study raises many new questions. How does GAPDH obtain mitochondrial heme? Mitochondrial and endoplasmic reticulum heme exporters have recently been identified (33, 34) and can now be tested to see whether they participate in upstream heme delivery to GAPDH. Why is Hsp90 needed for the sGC $\beta$  heme insertion process in cells? Hsp90 was not needed in our experiment documenting *in vitro* heme transfer from purified GAPDH to apo-sGC $\beta$ , despite firm evidence that in-cell sGC $\beta$  heme insertion is Hsp90-dependent and requires Hsp90 to form a direct complex with apo-sGC $\beta$  (19, 25, 34). What other cellular factors may regulate GAPDH heme delivery? It is possible that other cell proteins or small molecules may alter the heme affinity of GAPDH or its protein interactions to promote or inhibit heme delivery. One factor that may be involved is NO, which can modify GAPDH function through S-nitrosation of its Cys residues (35, 36) and can positively or negatively impact heme delivery to sGC (16, 37) and to several other heme proteins (38, 39). Finally, which proteins undergo GAPDH-dependent versus GAPDH-independent heme delivery? This study provides a general approach to address this question. Exploring these and other facets will lead to a better understanding of cell heme allocation and its role in governing heme protein maturation in health and disease.

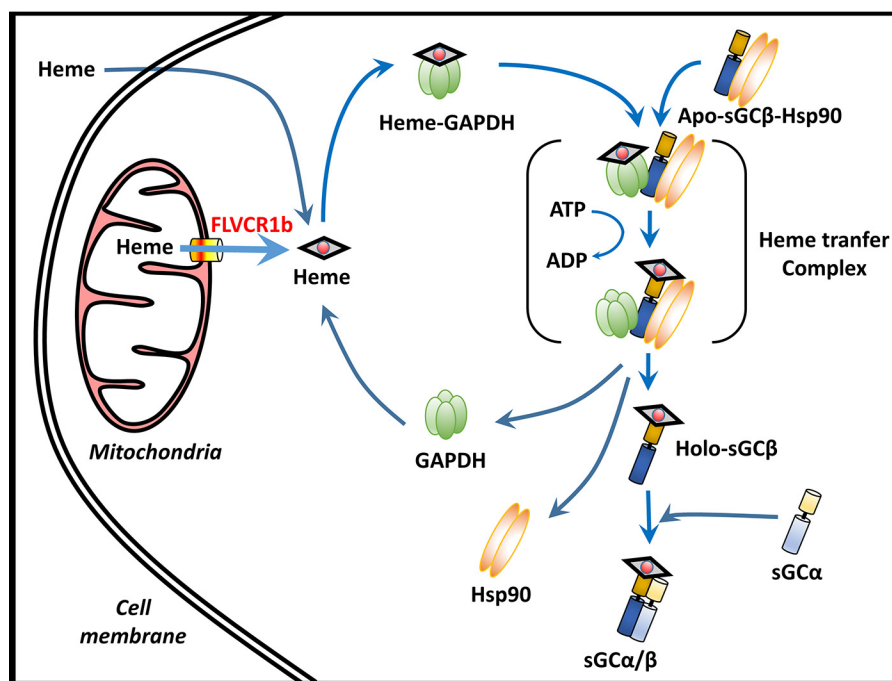


**Figure 7. Model of GAPDH-dependent sGC maturation in cells.** Mitochondrial heme or exogenous heme enters the cell cytosol and binds to the GAPDH tetramer to form a GAPDH–heme complex. This species then binds to the apo-sGC $\beta$ –Hsp90 complex, heme transfer and insertion into apo-sGC $\beta$  occur, and the proteins dissociate. The holo-sGC $\beta$  subunit then binds with an sGC $\alpha$  partner to create the mature and functional sGC heterodimer. See text for further details.

## Experimental procedures

### General methods and materials

The TC-FLAsH In-Cell Tetra Cysteine Tag Detection Kit was obtained from Invitrogen. All other reagents and materials were obtained from sources reported elsewhere.

### Molecular biology

pCMV5 mammalian expression plasmids containing rat sGC $\alpha$ 1(1–690), sGC $\beta$ 1(1–619), or sGC $\beta$ 1(1–619) with a tetra-cysteine motif (CCPGCC) at residue 239–244 have been reported previously (19). pcDNA3.1 plasmids containing HA-tagged human GAPDH WT and H53A have been reported previously (17). pcDNA3.1 plasmids encoding HA-tagged human GAPDH WT or H53A that are resistant to GAPDH siRNA (Dharmacon, Lafayette, CO, USA) were made by incorporating five silent mutations at the region that siRNA targets with primers listed in Table S1 and using Q5 High-Fidelity DNA Polymerase (New England Biolabs, Ipswich, MA, USA), using pcDNA3.1-GAPDH WT and H53A as templates. The pET20b vector containing rat sGC $\beta$ 1(1–385) with a C-terminal His<sub>6</sub> tag was a generous gift from Dr. Michael Marletta (University of California, Berkeley, CA, USA). Rat sGC $\beta$ 1(1–385) with a tetra-cysteine motif (CCPGCC) at residue 239–244 (TC-sGC $\beta$ 1(1–385)) was made with primers listed in Table S1 and Q5 High-Fidelity DNA Polymerase, using rat sGC $\beta$ 1(1–385) as templates. Rat TC-sGC $\beta$ 1(1–385) Y135A R139A (heme-binding variant) (28) was made with primers listed in Table S1 and Q5 High-Fidelity DNA Polymerase, using rat TC-sGC $\beta$ 1(1–385) as a template. The pcDNA3.1-eGFP-HS1 construct encoding the eGFP-mKATE2 heme sensor protein was a gift from Dr. Amit R. Reddi (Georgia Tech, Atlanta, GA, USA).

Sequencing of all constructs was done by Eurofins Genomics (Louisville, KY, USA).

### Protein purification

His<sub>6</sub>-tagged rat sGC $\beta$ 1(1–385) and GST-tagged human GAPDH were expressed in *Escherichia coli* BL21(DE3) and purified using methods reported previously (19, 29).

### Antibodies and siRNA

The primary antibodies for Western blotting were as follows: mouse monoclonal human GAPDH antibody (Santa Cruz Biotechnology, sc-32233, 1:1000), polyclonal sGC $\beta$ 1 antibody (Cayman Chemicals, 160897, 1:1000), polyclonal human Hsp90 antibody (Cell Signaling Technology, Danvers, MA, USA; 4874, 1:500), mouse monoclonal  $\beta$ -actin antibody (Sigma-Aldrich, 127M4857V, 1:1000), and mouse monoclonal HA-tag antibody (Sigma-Aldrich, 127M4869V, 1:500). The same sGC antibody was also used for IP at 1:100. Goat anti-mouse IgG (H + L)-HRP conjugate (Bio-Rad, 1706516, 1:1000) was used as a secondary antibody for Western blots. The Western Lightning Plus-ECL kit from PerkinElmer Life Sciences (Waltham, MA, USA) was used to visualize the proteins. ON-TARGETplus GAPDH siRNA was purchased from Dharmacon.

### Cell culture and transient transfection

HEK293 cells were cultured on fluorescent 96-well plates or on 10-cm dishes as described elsewhere (19). TC-sGC $\beta$ 1(1–619) and HA-GAPDH WT and mutant proteins were transfected into HEK293 cells using a method reported previously (19). GAPDH knockdown was performed using GAPDH siRNA according to a method reported previously (29). In some cases,

## GAPDH delivers heme to sGC

the heme biosynthesis inhibitor succinyl acetone was added at 400  $\mu\text{M}$  72 h prior to transfection to enable cell accumulation of apo-sGC $\beta$ (1–619) (19).

### IP and Western blot analysis

IP of sGC $\beta$  was performed using a method reported previously (19). Briefly, anti-sGC $\beta$  antibody was used to IP its bound proteins in HEK293 cell supernatant using protein G beads. GAPDH and Hsp90 were then probed using the respective antibodies. PAGE and Western blot analysis were performed using standard procedures. Band intensities were quantified using ImageJ (National Institutes of Health). Two-tailed Student's *t* test was performed to compare band intensities obtained from three independent experiments using a 95% confidence interval.

### In-cell FIAsh labeling of TC-sGC $\beta$ (1–619) and in vitro FIAsh labeling of TC-sGC $\beta$ (1–385) proteins

TC-sGC $\beta$ (1–619) expressed in HEK293 cells was labeled with the TC-FIAsh In-Cell Tetra Cysteine Tag Detection Kit (Invitrogen) using a method reported previously (19). Purified TC-sGC $\beta$ (1–385) and TC-sGC $\beta$ (1–385) Y135A/R139A were labeled with the TC-FIAsh In-Cell Tetra Cysteine Tag Detection Kit using a method published elsewhere (40).

### Monitoring heme insertion into sGC $\beta$ (1–619) in cells

Heme insertion into FIAsh-labeled TC-sGC $\beta$ (1–619) expressed in cells was monitored at 37 °C on a Flexstation3 96-well plate reader instrument (San Jose, CA) as reported previously (19).

### Monitoring heme transfer from GAPDH to sGC $\beta$ (1–385) in vitro

The heme–GAPDH complex was made by a method described previously (41) with modifications. Briefly, 25  $\mu\text{M}$  GAPDH tetramer in 4-(2-hydroxyethyl)-1-piperazinepropane-sulfonic acid buffer (40 mM (pH 7.6), 150 mM NaCl) was incubated with 30  $\mu\text{M}$  hemin for 15 min at room temperature. The mixture was then passed through a PD10 column to remove unbound heme. To monitor heme transfer from GAPDH to FIAsh-TC-sGC $\beta$ (1–385) proteins, 5  $\mu\text{M}$  heme–GAPDH tetramer was added to 5  $\mu\text{M}$  FIAsh-TC-sGC $\beta$ (1–385) in a fluorescence cuvette, and fluorescence emission was monitored over time at 25 °C in a Hitachi F2500 fluorescence spectrophotometer (Hitachi, Harrodsburg, KY, USA) with excitation/emission set at 508 nm and 528 nm, respectively. The resulting curves were fit to a first-order exponential equation in Origin Lab 8.0 (Origin Lab Corp., Northampton, MA, USA) to calculate the rates of fluorescence emission change.

### Detecting the labile heme level in cells

The composition of the eGFP-HS1 heme sensor and its use was as described previously (17, 22). Briefly, HEK293 cells cultured in DMEM with high glucose and FBS (10%) were transfected with pcDNA3.1-eGFP-HS1 using Lipofectamine 2000 (Thermo Fisher Scientific, Waltham, MA, USA). After 16 h, the medium was replaced, and cells were treated with medium containing nothing, heme (5  $\mu\text{M}$ ), or  $\delta$ -ALA (500  $\mu\text{M}$ ) + Fe-cit (200

$\mu\text{M}$ ) for 3 h. Cells were removed from the dish, washed with PBS, and resuspended in PBS + glucose. mKATE2-positive cells ( $1 \times 10^6$  per condition) were analyzed for the intensity of their GFP and mKATE2 fluorescence on a BD LSRFortessa instrument (BD Biosciences) (mKATE2 excitation 588 nm, emission 620 nm; GFP excitation 488 nm, emission 510 nm). Data were analyzed using FlowJo v10 (BD Biosciences) and presented as the ratio of GFP:mKATE2 fluorescence in cells *versus* cell number.

### cGMP ELISA

cGMP formation and its concentration in cell supernatant assays was determined by a method described previously (19) using a cGMP ELISA kit (Cell Signaling Technology). Two-tailed Student's *t* test was performed to compare activities obtained from three independent experiments using a 95% confidence interval.

### Fluorescence polarization measurements

FITC labeling of purified sGC $\beta$ (1–385) proteins and residual fluorescence polarization measurements were performed at room temperature using methods described previously (42).

### Data availability

All data are contained within the article.

**Acknowledgments**—We thank Dr. Andreas Papapetropoulos (University of Athens Medical School, Athens, Greece) for providing the pCMV5-sGC $\alpha$ 1 and pCMV5-sGC $\beta$ 1 constructs and BAY58–2267, Dr. Michael Marletta (University of California, Berkeley) for the sGC $\beta$  bacterial expression construct, and Dr. Amit Reddi (Georgia Institute of Technology, Atlanta) for the pcDNA3.1-eGFP-HS1 heme sensor construct.

**Author contributions**—Y. D., A. G., and D. J. S. conceptualization; Y. D. and S. S. data curation; Y. D. software; Y. D. formal analysis; Y. D. and D. J. S. validation; Y. D. and S. S. investigation; Y. D. visualization; Y. D., E. A. S., A. G., and D. J. S. methodology; Y. D. writing-original draft; Y. D., E. A. S., and D. J. S. writing-review and editing; D. J. S. resources; D. J. S. supervision; D. J. S. project administration.

**Funding and additional information**—This work was supported by NHLBI, National Institutes of Health Grants P01HL081064 and P01HL103453 (to D. J. S.), and K99HL144921 (to E. A. S.). The content is solely the responsibility of the authors and does not necessarily represent the official views of the National Institutes of Health.

**Conflict of interest**—The authors declare that they have no conflicts of interest with the contents of this article.

**Abbreviations**—The abbreviations used are: sGC, soluble guanylyl cyclase; TC, tetra-cysteine; SA, succinyl acetone; Fe-cit, ferric citrate;  $\delta$ -ALA, 5-aminolevulinic acid; eGFP, enhanced GFP; BAY58, BAY58-2667; IP, immunoprecipitation; HD, heme binding–deficient; iNOS, inducible nitric oxide synthase.

### References

1. Murad, F. (2008) Nitric oxide and cyclic guanosine monophosphate signaling in the eye. *Can. J. Ophthalmol.* **43**, 291–294 [CrossRef Medline](#)



2. Denninger, J. W., and Marletta, M. A. (1999) Guanylate cyclase and the NO/cGMP signaling pathway. *Biochim. Biophys. Acta* **1411**, 334–350 [CrossRef Medline](#)
3. Friebe, A., Sandner, P., and Schmidtko, A. (2020) cGMP: a unique 2nd messenger molecule: recent developments in cGMP research and development. *Naunyn Schmiedebergs Arch. Pharmacol.* **393**, 287–302 [CrossRef Medline](#)
4. Stasch, J. P., Pacher, P., and Evgenov, O. V. (2011) Soluble guanylate cyclase as an emerging therapeutic target in cardiopulmonary disease. *Circulation* **123**, 2263–2273 [CrossRef Medline](#)
5. Stasch, J. P., and Evgenov, O. V. (2013) Soluble guanylate cyclase stimulators in pulmonary hypertension. *Handb. Exp. Pharmacol.* **218**, 279–313 [CrossRef Medline](#)
6. Ben Aissa, M., Lee, S. H., Bennett, B. M., and Thatcher, G. R. (2016) Targeting NO/cGMP signaling in the CNS for neurodegeneration and Alzheimer's disease. *Curr. Med. Chem.* **23**, 2770–2788 [CrossRef Medline](#)
7. Montfort, W. R., Wales, J. A., and Weichsel, A. (2017) Structure and activation of soluble guanylyl cyclase, the nitric oxide sensor. *Antioxid. Redox Signal.* **26**, 107–121 [CrossRef Medline](#)
8. Horst, B. G., Yokom, A. L., Rosenberg, D. J., Morris, K. L., Hammel, M., Hurley, J. H., and Marletta, M. A. (2019) Allosteric activation of the nitric oxide receptor soluble guanylate cyclase mapped by cryo-electron microscopy. *Elife* **8**, e50634 [CrossRef Medline](#)
9. Kang, Y., Liu, R., Wu, J. X., and Chen, L. (2019) Structural insights into the mechanism of human soluble guanylate cyclase. *Nature* **574**, 206–210 [CrossRef Medline](#)
10. Childers, K. C., Yao, X. Q., Giannakoulis, S., Amason, J., Hamelberg, D., and Garcin, E. D. (2019) Synergistic mutations in soluble guanylyl cyclase (sGC) reveal a key role for interfacial regions in the sGC activation mechanism. *J. Biol. Chem.* **294**, 18451–18464 [CrossRef Medline](#)
11. Beuve, A. (2019) Wedging open a catalytic site. *Elife* **8**, e52418 [CrossRef Medline](#)
12. Ghosh, A., and Stuehr, D. J. (2017) Regulation of sGC via hsp90, cellular heme, sGC agonists, and NO: new pathways and clinical perspectives. *Antioxid. Redox Signal.* **26**, 182–190 [CrossRef Medline](#)
13. Martin, E., Berka, V., Tsai, A. L., and Murad, F. (2005) Soluble guanylyl cyclase: the nitric oxide receptor. *Methods Enzymol.* **396**, 478–492 [CrossRef Medline](#)
14. Rahaman, M. M., Nguyen, A. T., Miller, M. P., Hahn, S. A., Sparacino-Watkins, C., Jobbagy, S., Carew, N. T., Cantu-Medellin, N., Wood, K. C., Baty, C. J., Schopfer, F. J., Kelley, E. E., Gladwin, M. T., Martin, E., and Straub, A. C. (2017) Cytochrome b5 reductase 3 modulates soluble guanylate cyclase redox state and cGMP signaling. *Circ. Res.* **121**, 137–148 [CrossRef Medline](#)
15. Dai, Y., Haque, M. M., and Stuehr, D. J. (2017) Restricting the conformational freedom of the neuronal nitric-oxide synthase flavoprotein domain reveals impact on electron transfer and catalysis. *J. Biol. Chem.* **292**, 6753–6764 [CrossRef Medline](#)
16. Ghosh, A., Stasch, J. P., Papapetropoulos, A., and Stuehr, D. J. (2014) Nitric oxide and heat shock protein 90 activate soluble guanylate cyclase by driving rapid change in its subunit interactions and heme content. *J. Biol. Chem.* **289**, 15259–15271 [CrossRef Medline](#)
17. Sweeny, E. A., Singh, A. B., Chakravarti, R., Martinez-Guzman, O., Saini, A., Haque, M. M., Garee, G., Dans, P. D., Hannibal, L., Reddi, A. R., and Stuehr, D. J. (2018) Glyceraldehyde-3-phosphate dehydrogenase is a chaperone that allocates labile heme in cells. *J. Biol. Chem.* **293**, 14557–14568 [CrossRef Medline](#)
18. Hoffmann, L. S., Schmidt, P. M., Keim, Y., Hoffmann, C., Schmidt, H. H., and Stasch, J. P. (2011) Fluorescence dequenching makes haem-free soluble guanylate cyclase detectable in living cells. *PLoS ONE* **6**, e23596 [CrossRef Medline](#)
19. Dai, Y., Schlanger, S., Haque, M. M., Misra, S., and Stuehr, D. J. (2019) Heat shock protein 90 regulates soluble guanylyl cyclase maturation by a dual mechanism. *J. Biol. Chem.* **294**, 12880–12891 [CrossRef Medline](#)
20. Schultz, I. J., Chen, C., Paw, B. H., and Hamza, I. (2010) Iron and porphyrin trafficking in heme biogenesis. *J. Biol. Chem.* **285**, 26753–26759 [CrossRef Medline](#)
21. Gardner, L. C., Smith, S. J., and Cox, T. M. (1991) Biosynthesis of  $\delta$ -aminolevulinic acid and the regulation of heme formation by immature erythroid cells in man. *J. Biol. Chem.* **266**, 22010–22018 [Medline](#)
22. Hanna, D. A., Harvey, R. M., Martinez-Guzman, O., Yuan, X., Chandrasekharan, B., Raju, G., Outten, F. W., Hamza, I., and Reddi, A. R. (2016) Heme dynamics and trafficking factors revealed by genetically encoded fluorescent heme sensors. *Proc. Natl. Acad. Sci. U.S.A.* **113**, 7539–7544 [CrossRef Medline](#)
23. Hanna, D. A., Hu, R., Kim, H., Martinez-Guzman, O., Torres, M. P., and Reddi, A. R. (2018) Heme bioavailability and signaling in response to stress in yeast cells. *J. Biol. Chem.* **293**, 12378–12393 [CrossRef Medline](#)
24. Stasch, J. P., Schmidt, P. M., Nedvetsky, P. I., Nedvetskaya, T. Y., HS, S. A. K., Meurer, S., Deile, M., Taye, A., Knorr, A., Lapp, H., Müller, H., Turgay, Y., Rothkegel, C., Tersteegen, A., Kemp-Harper, B., Müller-Esterl, W., and Schmidt, H. H. (2006) Targeting the heme-oxidized nitric oxide receptor for selective vasodilatation of diseased blood vessels. *J. Clin. Invest.* **116**, 2552–2561 [CrossRef Medline](#)
25. Ghosh, A., and Stuehr, D. J. (2012) Soluble guanylyl cyclase requires heat shock protein 90 for heme insertion during maturation of the NO-active enzyme. *Proc. Natl. Acad. Sci. U.S.A.* **109**, 12998–13003 [CrossRef Medline](#)
26. Kollau, A., Opelt, M., Wölkart, G., Gorren, A. C. F., Russwurm, M., Koesling, D., Mayer, B., and Schrammel, A. (2018) Irreversible activation and stabilization of soluble guanylate cyclase by the protoporphyrin IX mimetic cinaciguat. *Mol. Pharmacol.* **93**, 73–78 [CrossRef Medline](#)
27. Ghosh, A., Koziol-White, C. J., Asosingh, K., Cheng, G., Ruple, L., Gronenberg, D., Friebe, A., Comhair, S. A., Stasch, J. P., Panettieri, R. A., Jr., Aronica, M. A., Erzurum, S. C., and Stuehr, D. J. (2016) Soluble guanylate cyclase as an alternative target for bronchodilator therapy in asthma. *Proc. Natl. Acad. Sci. U.S.A.* **113**, E2355–2362 [CrossRef Medline](#)
28. Hoffmann, L. S., Schmidt, P. M., Keim, Y., Schaefer, S., Schmidt, H. H., and Stasch, J. P. (2009) Distinct molecular requirements for activation or stabilization of soluble guanylyl cyclase upon haem oxidation-induced degradation. *Br. J. Pharmacol.* **157**, 781–795 [CrossRef Medline](#)
29. Chakravarti, R., Aulak, K. S., Fox, P. L., and Stuehr, D. J. (2010) GAPDH regulates cellular heme insertion into inducible nitric oxide synthase. *Proc. Natl. Acad. Sci. U.S.A.* **107**, 18004–18009 [CrossRef Medline](#)
30. Zhong, F., Pan, J., Liu, X., Wang, H., Ying, T., Su, J., Huang, Z. X., and Tan, X. (2011) A novel insight into the heme and NO/CO binding mechanism of the  $\alpha$  subunit of human soluble guanylate cyclase. *J. Biol. Inorg. Chem.* **16**, 1227–1239 [CrossRef Medline](#)
31. Fritz, B. G., Hu, X., Brailey, J. L., Berry, R. E., Walker, F. A., and Montfort, W. R. (2011) Oxidation and loss of heme in soluble guanylyl cyclase from *Manduca sexta*. *Biochemistry* **50**, 5813–5815 [CrossRef Medline](#)
32. Surmeli, N. B., and Marletta, M. A. (2012) Insight into the rescue of oxidized soluble guanylate cyclase by the activator cinaciguat. *Chembiochem.* **13**, 977–981 [CrossRef Medline](#)
33. Chiabrando, D., Marro, S., Mercurio, S., Giorgi, C., Petrillo, S., Vinchi, F., Fiorito, V., Fagoonee, S., Camporeale, A., Turco, E., Merlo, G. R., Silengo, L., Altruda, F., Pinton, P., and Tolosano, E. (2012) The mitochondrial heme exporter FLVCR1b mediates erythroid differentiation. *J. Clin. Invest.* **122**, 4569–4579 [CrossRef Medline](#)
34. Galmozzi, A., Kok, B. P., Kim, A. S., Montenegro-Burke, J. R., Lee, J. Y., Spreafico, R., Masure, S., Albert, V., Cintron-Colon, R., Godio, C., Webb, W. R., Conti, B., Solt, L. A., Kojetin, D., Parker, C. G., et al. (2019) PGRMC2 is an intracellular haem chaperone critical for adipocyte function. *Nature* **576**, 138–142 [CrossRef Medline](#)
35. Chakravarti, R., and Stuehr, D. J. (2012) Thioredoxin-1 regulates cellular heme insertion by controlling S-nitrosation of glyceraldehyde-3-phosphate dehydrogenase. *J. Biol. Chem.* **287**, 16179–16186 [CrossRef Medline](#)
36. Jia, J., Arif, A., Terenzi, F., Willard, B., Plow, E. F., Hazen, S. L., and Fox, P. L. (2014) Target-selective protein S-nitrosylation by sequence motif recognition. *Cell* **159**, 623–634 [CrossRef Medline](#)
37. Ignarro, L. J., Adams, J. B., Horwitz, P. M., and Wood, K. S. (1986) Activation of soluble guanylate cyclase by NO-hemoproteins involves NO-heme exchange: comparison of heme-containing and heme-deficient enzyme forms. *J. Biol. Chem.* **261**, 4997–5002 [Medline](#)
38. Waheed, S. M., Ghosh, A., Chakravarti, R., Biswas, A., Haque, M. M., Panda, K., and Stuehr, D. J. (2010) Nitric oxide blocks cellular heme inser-

## GAPDH delivers heme to sGC

- tion into a broad range of heme proteins. *Free Radic. Biol. Med.* **48**, 1548–1558 [CrossRef Medline](#)
39. Kim, Y. M., Bergonia, H. A., Müller, C., Pitt, B. R., Watkins, W. D., and Lancaster, J. R., Jr. (1995) Nitric oxide and intracellular heme. *Adv. Pharmacol.* **34**, 277–291 [CrossRef Medline](#)
40. Pan, J., Yuan, H., Zhang, X., Zhang, H., Xu, Q., Zhou, Y., Tan, L., Nagawa, S., Huang, Z. X., and Tan, X. (2017) Probing the molecular mechanism of human soluble guanylate cyclase activation by NO *in vitro* and *in vivo*. *Sci. Rep.* **7**, 43112 [CrossRef Medline](#)
41. Hannibal, L., Collins, D., Brassard, J., Chakravarti, R., Vempati, R., Dorlet, P., Santolini, J., Dawson, J. H., and Stuehr, D. J. (2012) Heme binding properties of glyceraldehyde-3-phosphate dehydrogenase. *Biochemistry* **51**, 8514–8529 [CrossRef Medline](#)
42. Sarkar, A., Dai, Y., Haque, M. M., Seeger, F., Ghosh, A., Garcin, E. D., Montfort, W. R., Hazen, S. L., Misra, S., and Stuehr, D. J. (2015) Heat shock protein 90 associates with the Per-Arnt-Sim domain of heme-free soluble guanylate cyclase: implications for enzyme maturation. *J. Biol. Chem.* **290**, 21615–21628 [CrossRef Medline](#)